UNIVERSITY
OF TRENTO

DIPARTIMENTO DI INGEGNERIA E SCIENZA DELL'INFORMAZIONE

38123 Povo – Trento (Italy), Via Sommarive 14
http://www.disi.unitn.it

FULLY-INTERLEAVED LINEAR ARRAYS WITH PREDICTABLE SIDELOBES BASED ON ALMOST DIFFERENCE SETS

G. Oliveri, and A. Massa

January 2011

Technical Report # DISI-11-092

Fully-Interleaved Linear Arrays with Predictable Sidelobes based on Almost Difference Sets

G. Oliveri and A. Massa

ELEDIA Research Group

Department of Information and Communication Technologies,

University of Trento, Via Sommarive 14, 38050 Trento - Italy

Tel. +39 0461 882057, Fax +39 0461 882093

E-mail: *andrea.massa@ing.unitn.it, giacomo.oliveri@dit.unitn.it*

Web-site: *http://www.eledia.ing.unitn.it*

Fully-Interleaved Linear Arrays with Predictable Sidelobes based on Almost Difference Sets

G. Oliveri and A. Massa

Abstract

This paper proposes an analytical technique based on Almost Difference Sets (ADSs) for the design of interleaved linear arrays with well-behaved and predictable radiation features. Thanks to the mathematical properties of ADSs, such a methodology allows the design of interlaced arrangements with peak sidelobe levels (PSLs) only dependent on the aperture size, the number of elements of each subarray, and the behavior of the autocorrelation function of the ADS at hand. PSL bounds are analytically derived and an extensive numerical validation is provided to assess the reliability, the computational efficiency, and the effectiveness of the proposed approach. It is worth noticing that, although without any optimization, such an analytic technique si still able to improve (on average $0.3\,dB$) the performances of GA-optimized layouts.

Key words: Array Antennas, Interleaved Arrays, Linear Arrays, Almost Difference Sets, Sidelobe Control.

1 Introduction

Shared aperture antennas are of great interest in modern wireless systems for communications, detection, location, and remote sensing because of the need to realize multiple functions in a limited space [1]. In this framework, aperture arrays of intermixed elements (often indicated as interleaved, interlaced or interspread arrays) provide interesting performances in terms of hardware complexity, aperture efficiency, and flexibility [1]. However, each array of an interleaved arrangement usually shows a lower gain and a higher peak sidelobe level (PSL) than the corresponding non-interlaced design [2].

In order to overcome such drawbacks, several approaches have been proposed [1][2][3][4] starting from random techniques aimed at reducing the PSL of shared apertures [5]. More recently, stochastic optimization techniques [1][2] or hybrid approaches [6] have been successfully applied. Despite their effectiveness, statistical methodologies are computationally inefficient when dealing with large apertures and *a-priori* estimates of the expected performances are usually not available.

In this paper, the problem of designing equally-weighted fully-interleaved arrays is addressed to provide design guidelines to be employed when, whether by choice or by necessity, a computationally inexpensive and sub-optimal solution with predictable performances is preferred to a random or a stochastically-optimized design. Towards this end, the synthesis of interleaved arrays is faced with an innovative approach that exploits the so-called Almost Difference Sets (ADSs). ADSs are binary sequences characterized by a three-level autocorrelation [7]. They constitute a generalization of Difference Sets [8] and have been used to design thinned arrays with predictable sidelobes [9]. In order to exploit ADSs for the synthesis of interleaved arrangements, let us consider the following properties:

- the complementary of an ADS is still an ADS [10];
- an ADS-based array has a low and predictable PSL [9];
- ADS arrangements can be analytically (i.e., without any optimization) designed whatever the aperture size [9].

Such features suggest the design of an interleaved array with low sidelobes by determining the memberships of the array elements to the two subarrays according to the sequence of 0s or 1s of an ADS sequence [11] in a complementary way.

Let also notice that an extension or application of the PSL estimators obtained in [9] for ADS-based thinned arrays to interleaved distributions is not trivial. As a matter of fact, the bounds deduced in [9] refer to the best thinned array among those obtained by cyclically shifting a reference ADS sequence. However, such a configuration is not generally the best one when shared apertures are of interest, since the complementary array can exhibit an unsatisfactory PSL. The definition of a compromise ADS guaranteeing the most suitable PSL for both arrays is then needed. Accordingly, a new theoretical and numerical analysis is mandatory to deduce and validate suitable bounds for ADS-based interleaved arrays.

The outline of the paper is as follows. After a short introduction on array thinning through ADSs (Sect. 2), the exploitation of the ADS properties for array interleaving is analyzed from a mathematical viewpoint to highlight the key features of ADS-based designs (Sect. 3). The numerical validation is carried out in Sect. 4 by considering a set of representative examples and comparisons with state-of-the art approaches. Finally, some conclusions are drawn (Sect. 5).

2 Almost Difference Sets in Linear Array Thinning

In this section, the ADS-based guidelines for linear array thinning [9] are briefly reviewed and the most relevant properties of ADSs discussed.

The array factor of a linear array defined over a lattice of N equally-spaced positions (d being the inter-element distance in wavelength) in the absence of mutual coupling is given by [13]

$$S_I(u) = \sum_{n=0}^{N-1} w_I(n) exp(i2\pi ndu) \tag{1}$$

where $w_I(n)$ is the array weight of the n-th element, $u = sin(\theta)$ ($u \in [-1, 1]$). Dealing with equally-weighted thinned arrays, $w_I(n)$ can either assume the value 1 (i.e., the radiating element is present) or 0 (i.e., the element is missing). In [9], the design of thinned arrays is carried out

according to the following rule

$$w_I(n) = \begin{cases} 1 & if\, n \in \mathbf{D}_I \\ 0 & otherwise \end{cases}$$

where $\mathbf{D}_I$ is an (N, K, Λ, t)-ADS, that is a set of K unique integers belonging to the range $[0, N-1]$ whose associated binary sequence, $w_I(n)$, $n = 0, .., N-1$ has a three-valued cyclic autocorrelation function $\xi_I(\tau) \triangleq \sum_{n=0}^{N-1} w_I(n) w_I\left[(n+\tau)|_{mod\, N}\right]$, $\tau \in [0,\ N-1]$, of period N

$$\xi_I(\tau) = \begin{cases} K & \tau = 0 \\ \Lambda & for\, t\, values\, of\, \tau \\ \Lambda + 1 & otherwise \end{cases} \tag{2}$$

Thanks to this, it is possible to predict the behavior of the power pattern of the resulting thinned arrangement. As a matter of fact, it can be shown that [9] the inverse discrete Fourier transform ($IDFT$) of $\xi_I(\tau)$, $\Xi_I(k) \triangleq \sum_{\tau=0}^{N-1} \xi_I(\tau)\, exp\left(2\pi i \frac{\tau k}{N}\right)$, is equal to the samples of the array power pattern $|S_I(u)|^2$ at $u = \frac{k}{dN}$

$$\Xi_I(k) = \left| S_I\left(\frac{k}{dN}\right)\right|^2. \tag{3}$$

By exploiting such a property, it has been possible [9] to determine suitable bounds for the peak sidelobe level of the ADS-based arrays

$$PSL_{MIN}^{opt} \leq PSL_{DW}^{opt} \leq PSL^{opt}\left\{\mathbf{D}_I\right\} \leq PSL_{UP}^{opt} \leq PSL_{MAX}^{opt} \tag{4}$$

where

$$PSL_{opt}\left\{\mathbf{D}_I\right\} = min_{\sigma \in [0, N-1]}\left\{PSL\left(\mathbf{D}_I^{(\sigma)}\right)\right\}, \tag{5}$$

$\mathbf{D}_I^{(\sigma)} \triangleq \left\{d_k^{(\sigma)} \in \mathbb{Z}^N, k = 1, ..., K :\ d_k^{(\sigma)} = (d_k + \sigma)|_{mod\, N}\right\}$ being the σ-th sequence obtained by cyclically shifting of σ positions the original ADS $\mathbf{D}_I$ ($\mathbf{D}_I^{(\sigma)}$ is still an ADS [7]) and

$$PSL\left(\mathbf{D}_I^{(\sigma)}\right) \triangleq \frac{max_{u \notin R_m} |S_I(u)|^2}{|S_I(0)|^2}, \tag{6}$$

where $R_M \triangleq \left\{ -U_M \leq u \leq U_M,\, U_M = \frac{1}{2Nd\sqrt{\frac{max_k \Xi(k)}{\Xi(0)}}} \right\}$ is the mainlobe region [9]. Moreover,

$$\begin{cases} PSL_{MIN}^{opt} = \frac{K-\Lambda-1-\sqrt{\frac{t(N-t)}{(N-1)}}}{(N-1)\Lambda+K-1+N-t} \\ PSL_{DW}^{opt} = \frac{max_k \Xi_I(k)}{\Xi_I(0)} \\ PSL_{UP}^{opt} = \frac{max_k \Xi_I(k)}{\Xi_I(0)} \left(0.8488 + 1.128\, log_{10} N\right) \\ PSL_{MAX}^{opt} = \frac{\left(K-\Lambda-1+\sqrt{t(N-t)}\right)(0.8488+1.128\, log_{10} N)}{(N-1)\Lambda+K-1+N-t}. \end{cases}$$

Properties and theorems of ADSs can be found in [7][10] and the references therein. In the next section, the properties of ADSs and the associated arrangements will be exploited for designing interleaved arrays.

3 ADS-Interleaved Arrays - Mathematical Formulation

Let us consider the following theorem:

> *Theorem 1* [10]: if $\mathbf{D}_I$ is an ADS, then its complementary set $\mathbf{D}_C \triangleq \mathbb{Z}^N \backslash \mathbf{D}_I$, (i.e., $\mathbf{D}_C = \left\{ d_j \in \mathbb{Z}^N,\, j = 1, ..., N-K :\, d_j \notin \mathbf{D}_I \right\}$) is an (N, K_C, Λ_C, t)-ADS, where $K_C = N - K$ and $\Lambda_C = N - 2K + \Lambda$[(1)].

Starting from an ADS array with weights $w_I(n)$, $n = 0, .., N-1$, the coefficients $w_C(n)$ of the complementary distribution are given by

$$w_C(n) = 1 - w_I(n),\;\; n = 0, .., N-1. \tag{7}$$

The aperture efficiency η_{ap} ($\eta_{ap} \triangleq \frac{\sum_{n=0}^{N-1} w_I(n) + \sum_{n=0}^{N-1} w_C(n)}{N}$) of the arising *fully interleaved array* turns out to be $\eta_{ap} = \frac{K+K_C}{N}$ [1] and it is equal to 1 since $K_C = N - K$ (see Theorem 1).
For illustrative purposes, let us consider the $(30, 15, 7, 22)$-ADS [11]

$$\mathbf{D}_I = \{5, 6, 8, 9, 10, 14, 16, 17, 19, 20, 22, 23, 24, 27, 29\} \tag{8}$$

(1) It is worth to point out that *Theorem 1* holds true also for a sub-class of ADSs for which $t = 0$ or $t = N-1$ [12] [namely, the Difference Sets (DSs)] widely used in array thinning [8].

whose complementary ADS is given by

$$\mathbf{D}_C = \{0, 1, 2, 3, 4, 7, 11, 12, 13, 15, 18, 21, 25, 26, 28\}. \tag{9}$$

The associated binary sequences, $w_I(n)$ and $w_C(n)$, $n = 0, ..., N-1$, and the interleaved arrangement are shown in Fig. 1(*a*).

Since the element distribution of the interleaved antenna is composed by two distinct ADS-based thinned arrays, several conclusions drawn in [9] still hold true. More specifically, (*a*) both arrays are expected to exhibit lower PSLs with respect to random arrangements, (*b*) each design can be cyclically shifted to obtain up to N different ADS arrangements, and (*c*) the methodology can be applied to synthesize extremely large apertures with negligible computational costs. Moreover, some specific properties of ADS interleaved arrays can be deduced from *Theorem 1*. As an example, the autocorrelation functions satisfy the following equation (see the Appendix)

$$\xi_C(\tau) = \xi_I(\tau) + [N(1-2\nu)] \tag{10}$$

where $\xi_C(\tau) \triangleq \sum_{n=0}^{N-1} w_C(n) w_C\left[(n+\tau)|_{mod\,N}\right]$ and $\nu \triangleq \frac{K}{N}$ is the unbalancing factor ($\nu \in [0, 0.5]$, $\nu = 0.5$ being the index value for interleaved arrays with the same number of active elements). For illustrative purposes, the plots of the autocorrelation functions of the ADSs in (8) and (9) are reported in Fig. 1(*b*). As expected, $\xi_I(\tau) = \xi_C(\tau)$ since $\nu = 0.5$. On the other hand, the samples of the corresponding power patterns $|S_I(u)|^2$ and $|S_C(u)|^2$ comply with Eq. (3)[(2)], and the ratio between the normalized values of $\Xi_I(k)$ and $\Xi_C(k)$, $\Psi(k) \triangleq \frac{\Xi_C(k)}{\Xi_C(0)} \frac{\Xi_I(0)}{\Xi_I(k)}$, is constant and equal to (see the Appendix)

$$\Psi = \left(\frac{1-\nu}{\nu}\right)^2 \qquad k = 1, ..., N-1 \tag{11}$$

[e.g., $\Psi = 0$ dB in Fig. 1(*c*) being $\nu = 0.5$]. In such a case, $\Xi_I(k) = \Xi_C(k)$ (i.e., the samples of the power patterns of the interleaved arrays at $u = \frac{k}{dN}$ coincide) since $\xi_I(\tau) = \xi_C(\tau)$.

[(2)] Eq. (3) can be written for the array deduced from $\mathbf{D}_C$ by replacing $\xi_I(\tau)$ with $\xi_C(\tau)$, $\Xi_I(k)$ with $\Xi_C(k) \triangleq IDFT\{\xi_C(\tau)\}$, and $S_I(u)$ with $S_C(u) \triangleq \sum_{n=0}^{N-1} w_C(n) exp(i2\pi ndu)$.

As for $\nu \neq 0.5$, the interleaved arrangement deduced from the $(53, 14, 3, 26)$-ADS [11] is displayed in Fig. 2(*a*). In this case, $\nu \approx 0.26$ and the interleaved subarrays have a quite different number of active elements. According to (10), $\xi_C(\tau)$ has the same behavior of $\xi_I(\tau)$, but it is a replica translated by $N(1-2\nu) = 25$ [Fig. 2(*b*)]. The pattern samples still coincide with the $IDFT$ values of the corresponding autocorrelations at $u = \frac{k}{dN}$, even though significantly differ from those when $\nu = 0.5$ since here $\Psi \approx 8.89$ dB [Fig. 2(*c*)]. As a matter of fact, non-negligible differences verify between the PSLs of $|S_I(u)|^2$ and $|S_C(u)|^2$ because of the dependence of Ψ on ν (Fig. 3).

As regards the PSL bounds of interleaved ADS-based arrays, a straightforward exploitation of (4) is not at hand. Indeed, although Eq. (4) can be applied to predict $PSL_{opt}\{\mathbf{D}_I\} = min_{\sigma\in[0,N-1]}\left\{PSL\left(\mathbf{D}_I^{(\sigma)}\right)\right\}$ or $PSL_{opt}\{\mathbf{D}_C\} = min_{\sigma\in[0,N-1]}\left\{PSL\left(\mathbf{D}_C^{(\sigma)}\right)\right\}$ [9], it is not generally possible to determine a shift optimal for both $\mathbf{D}_I$ and $\mathbf{D}_C$ since $\sigma_I^{opt} \neq \sigma_C^{opt}$ being $\sigma_I^{opt} \triangleq argmin_{\sigma\in[0,N-1]}\left\{PSL\left(\mathbf{D}_I^{(\sigma)}\right)\right\}$ and $\sigma_C^{opt} \triangleq argmin_{\sigma\in[0,N-1]}\left\{PSL\left(\mathbf{D}_C^{(\sigma)}\right)\right\}$. Therefore, a suitable compromise solution, which is not guaranteed to satisfy (4), has to be taken into account. However, since several "compromises" could be defined also according to the application at hand (e.g., different PSL constraints could be required on each subarray of the interleaved arrangement) and unlike [9], suitable PSL bounds for any admissible compromise interleaving (i.e., any value of σ) are defined (see the Appendix)

$$\begin{aligned} PSL_{MIN}^I \leq PSL_{DW}^I \leq PSL\left(\mathbf{D}_I^{(\sigma)}\right) \leq PSL_{UP}^I \leq PSL_{MAX}^I \\ PSL_{MIN}^C \leq PSL_{DW}^C \leq PSL\left(\mathbf{D}_C^{(\sigma)}\right) \leq PSL_{UP}^C \leq PSL_{MAX}^C \end{aligned} \tag{12}$$

where $PSL_{MIN}^I = PSL_{MIN}^{opt}$, $PSL_{DW}^I = \Gamma\left(0.5 + 0.8\,log_{10}N\right)$, $PSL_{UP}^I = \frac{max_k \Xi_I(k)}{\Xi_I(0)}\left(1.9 + 1.8\,log_{10}N\right)$, $PSL_{MAX}^I = \frac{\left(K-\Lambda-1+\sqrt{t(N-t)}\right)(1.9+1.8\,log_{10}N)}{K^2}$, and $PSL^C = \Psi PSL^I$, being

$$\Gamma \triangleq \frac{min_k\left(\Xi_I(k)\right)}{K^2} \quad k = 1, .., \left\lfloor \frac{N-1}{2} \right\rfloor. \tag{13}$$

It is worthwhile to point out that, while the values of PSL_{DW}^I and PSL_{UP}^I can be determined only when the explicit form of the ADS is available, the computation of PSL_{MAX}^I and PSL_{MIN}^I only requires the knowledge of N, K, Λ, and t. Moreover, one can observe that

mutual-coupling effects could be integrated in the above treatment by considering an analysis similar to that performed in [14] for thinned ADS arrangements.

4 Numerical Analysis and Validation

This section is aimed at numerically assessing the performances of interleaved arrays based on ADSs as well as the reliability of the *a-priori* bounds in (12). Such a study is carried out by considering numerical experiments concerned with arrays having different apertures and thinning factors [11].

The first numerical example deals with balanced interleaved arrays (i.e., $\nu = 0.5$) for which $\Psi = 1$. The plots of $PSL\left(\mathbf{D}_I^{(\sigma)}\right)$ and $PSL\left(\mathbf{D}_C^{(\sigma)}\right)$ versus σ in Fig. 4(*a*) refer to the interleaved arrangements generated from the $(150, 75, 37, 112)$-ADS ($N = 150$, $K = K_C = 75$, $\eta \triangleq \frac{t}{N-1} \approx 0.75$). As it can be observed, every interleaved configuration (i.e., different value of σ) presents a PSL value that complies with (12) [Fig. 4(*a*)]. On the other hand, a shift optimal for both sub-arrays cannot be identified since $\sigma_I^{opt} \neq \sigma_C^{opt}$ [Fig. 4(*a*)], although the power patterns in correspondence with

$$\sigma^{comp} \triangleq argmin_\sigma \left[PSL\left(\mathbf{D}_I^{(\sigma)}\right) + PSL\left(\mathbf{D}_C^{(\sigma)}\right)\right] \tag{14}$$

[Fig. 4(*b*)], σ_I^{opt} [Fig. 4(*c*)], and σ_C^{opt} [Fig. 4(*d*)] indicate that different compromise solutions (e.g., minimum PSL for either one or both the arrays) can be easily generated by simply cyclically shifting the reference ADS without any optimization.

Similar conclusions hold true also for different values of N and η as confirmed by the plots in Fig. 5 where the results concerned with the $(700, 350, 174, 175)$-ADS ($N = 700$, $K = K_C = 350$, $\eta \approx 0.25$) are shown. The existence of different compromise solutions within the *a-priori* bounds [indicated by the boxes in Figs. 6(*a*), 7(a), 10(*b*), and 11(*b*)] is further highlighted in Fig. 6(*a*) ($\nu = 0.5$, $\eta = 0.25$) for different aperture sizes ($N = 150,\ 312,\ 700$). As expected, wider arrays provide lower PSL values whatever the "compromise" criterion [Fig 6(*a*)] and, for each dimension N, there exist several arrangements with PSL performances close to those with σ_I^{opt}, σ_C^{opt}, and σ^{comp} [Fig. 6(*a*)]. This latter as well as the uniform distribution of the "representative"

points in Fig. 6(*a*) further confirm the flexibility and effectiveness of the ADS-based approach in determining a broad set of compromise alternatives by means of simple cyclic shifts of a reference sequence.

In order to complete the numerical validation for $\nu = 0.5$ and $\eta = 0.25$, Figure 6(*b*) summarizes the obtained results in terms of PSL versus N.

Although balanced arrangements (i.e., $\nu = 0.5$) are commonly analyzed in the literature [1] and usually adopted in practical applications, interleaved arrays with $\nu \neq 0.5$ can be of some interest when dealing with wireless services requiring at the same time different radiation performances on the same physical aperture. In order to analyze their performances, the values of the PSLs and their bounds are shown in Fig. 7 for different aperture sizes ($N = 149, 349, 701$) being $\nu = 0.25$ and $\eta = 0.5$. As it can be observed, $PSL\left(\mathbf{D}_I^{(\sigma)}\right)$ and $PSL\left(\mathbf{D}_C^{(\sigma)}\right)$ significantly differ [Fig. 7(*a*)] because of the unbalance between the two subarrays. Nevertheless, their values still comply with (12) as better resumed in Figs. 7(*b*)-7(*c*). For completeness, the power patterns in correspondence with σ^{comp} and for two representative cases are reported in Fig. 8 [Fig. 8(*a*) - $N = 149$, Fig. 8(*b*) - $N = 701$]. As expected, the envelopes of the patterns differ approximately by Ψ ($\Psi \approx 9.5$ dB) within the sidelobe region outside R_M.

Such a behaviour suggests the use of non-isotropic array elements to compensate the PSL differences between the two interleaved arrays then widening the admissible set of ADS-based interleaved arrays with similar/close radiation characteristics of their subarrays. To investigate such a possibility, a simple model for the elementary radiator is considered in the following. More specifically, a $cos^m(\theta)$-element is employed [15] (see Fig. 9) and the array pattern is modified as follows

$$S_I^{(m)}(u) = S_I(u) \times \left(\sqrt{1-u^2}\right)^m$$

being $\sqrt{1-u^2} = cos\theta$. For notation simplicity, let us indicate with $PSL\left(\mathbf{D}_I^{(\sigma)}, m\right) \triangleq \frac{max_{u \notin R_m}\left|S_I^{(m)}(u)\right|^2}{\left|S_I^{(m)}(0)\right|^2}$ the associated peak sidelobe level. By analyzing the behaviours of $PSL\left(\mathbf{D}_C^{(\sigma)}\right)$ and $PSL\left(\mathbf{D}_I^{(\sigma)}, m\right)$ ($m \leq 0.25$) of the interleaved array deduced from the $(106, 52, 25, 78)$-ADS [Fig. 10(*a*)], one can infer that the use of a very low-directivity radiator ($m \approx 0.25$) [i.e., a small "translation" of the representative points in Fig. 10(*b*)] is enough to reach the condition $PSL\left(\mathbf{D}_C^{(\sigma_m^{comp})}\right) \approx$

$PSL\left(\mathbf{D}_I^{(\sigma_m^{comp})}, m\right)$ [Fig. 10(*c*)] since $\Psi \approx 0.32$ dB for the ADS at hand. As a matter of fact, the value of m depends on Ψ. The larger Ψ, the higher is the directivity of the array element necessary to balance the radiation patterns of the two subarrays. As an example, the interleaved distribution generated from the $(109, 27, 6, 54)$-ADS ($\nu \approx 0.25$) and characterized by $\Psi \approx 9.64$ dB [Fig 11(*a*)] requires a higher m value (i.e., $m \approx 300$). The plots in Fig. 11(*b*) confirm that a larger translation is needed in this case to locate the point representative of σ_m^{comp} close to the diagonal of the diagram [i.e., the locus where $PSL\left(\mathbf{D}_C^{(\sigma^{comp})}\right) = PSL\left(\mathbf{D}_I^{(\sigma^{comp})}, m\right)$]. On the other hand, the use of a highly directive element significantly modifies the original ADS-based pattern as shown in Fig. 11(*c*) where the plots of the compromise patterns for different values of m are reported. It should be also noted that a more regular pattern could be synthesized by resorting to more complex or customized radiating elements and a suitable optimization for each ADS at hand, for the time being, out of the scope of the present paper.

The last experiment is aimed at comparing the performances of ADS-based interleaved designs with those from state-of-the-art GA-based approaches [1]. Towards this end, the benchmark arrangement described in [1] and characterized by $N = 60$ and $\nu = 0.5$ is dealt with. The PSL of the GA-optimized array [1] and those of the ADS-based designs based on the $(60, 30, 14, 15)$-ADS are shown in Figs. 12(*a*)-12(*b*). The corresponding beampatterns in Fig. 12(*c*) show that the ADS interleaved array favourably compares with the GA antenna [$PSL_{GA} = -13.48$ dB vs. $PSL\left(\mathbf{D}_I^{(\sigma^{comp})}\right) = -13.27$ dB and $PSL\left(\mathbf{D}_C^{(\sigma^{comp})}\right) = -13.93$ dB], even if no optimization has been performed for the ADS synthesis.

Moreover, Figure 12(*b*) points out that several shifted variations of the reference ADS provide PSL performances close to that of the GA-optimized array. This further confirms the convenience of exploiting (for a pre-screening of the admissible interleaved arrays or as starting point for optimization processes) the ADSs to synthesize reliable and efficient interleaved arrangements.

5 Conclusions

In this paper, an ADS-based methodology has been proposed for interleaving equally-weighted linear arrays operating on the same frequency band. Such a deterministic approach is not aimed at synthesizing optimal arrays, but rather to provide suitable guidelines for the efficient design of shared apertures with predictable performances. An extensive numerical analysis has been carried out to evaluate the PSL performances as well as to prove the reliability of the analytically-derived PSL bounds in the absence of mutual coupling effects.

The obtained results have pointed out the following key features of the ADS-based interleaving:

- the PSLs of the interleaved arrays are *a-priori* known when the corresponding reference ADS sequences are available in explicit form, while suitable bounds are predicted otherwise;
- the difference between the PSL bounds of the two complementary subarrays amounts to Ψ and only depends on the thinning index ν (i.e., $PSL^C = \Psi \times PSL^I$);
- the ADS-based approach can be straightforwardly applied to synthesize both balanced ($\nu = 0.5$) and unbalanced interleaved arrays ($\nu \rightarrow 0$);
- the ADS-based design enables the synthesis of very large interleaved arrays with negligible computational costs and resources;
- several compromise configurations that satisfy different requirements can be easily generated from a reference ADS by means of cyclic shifts;
- ADS interleaved arrays favourably compare with state-of-the-art optimized arrangements [e.g., $PSL_{GA} = -13.48$ dB vs. $PSL\left(\mathbf{D}_I^{(\sigma^{comp})}\right) = -13.27$ dB and $PSL\left(\mathbf{D}_C^{(\sigma^{comp})}\right) = -13.93$ dB], although the ADS synthesis does not include any optimization;
- directive elements can be profitably used to enlarge the applicability of ADSs as well as the number of admissible balanced arrays.

It is also worth observing that, although the proposed technique does not theoretically generate the optimal solution of the synthesis problem at hand, it can be easily integrated with optimiza-

tion approaches either to define a sub-optimal starting solution for a local search or to generate the initial population for a multiple-agent optimization.

Future efforts will be devoted to extend the ADS-based synthesis method to other array geometries and wireless scenarios, as well as to take into account the effects of mutual coupling between the array antennas in the mathematical derivation. Moreover, although out of the scope of this paper and not pertinent to array synthesis, but rather to combinatorial mathematics, advances in the generation techniques of ADSs are expected.

Appendix

***- Derivation of* (10)**

By definition

$$\xi_C(\tau) = \sum_{n=0}^{N-1} w_C(n) w_C\left[(n+\tau)|_{mod\,N}\right]. \tag{15}$$

By exploiting (7), it results that

$$\xi_C(\tau) = \sum_{n=0}^{N-1} \left[1 - w_I(n)\right]\left\{1 - w_I\left[(n+\tau)|_{mod\,N}\right]\right\}$$

and after simple manipulations, we obtain

$$\begin{aligned}\xi_C(\tau) &= \textstyle\sum_{n=0}^{N-1} 1 - \sum_{n=0}^{N-1} w_I(n) - \sum_{n=0}^{N-1} w_I\left[(n+\tau)|_{mod\,N}\right] + \sum_{n=0}^{N-1} w_I(n) w_I\left[(n+\tau)|_{mod\,N}\right] = \\ &= N - 2K + \xi_I(\tau).\end{aligned}$$

being $\sum_{n=0}^{N-1} w_I(n) = \sum_{n=0}^{N-1} w_I\left[(n+\tau)|_{mod\,N}\right] = K$.

***- Derivation of* (11)**

Starting from Eq. (10) and taking into account the definition of $\Xi_C(k)$, it can be shown that

$$\begin{aligned}\Xi_C(k) = &\ \textstyle\sum_{n=0}^{N-1} \xi_C(\tau) exp\left(2\pi i \frac{\tau k}{N}\right) = \\ = &\ \textstyle\sum_{n=0}^{N-1} \left\{\xi_I(\tau) + \left[N\left(1-2\nu\right)\right]\right\} exp\left(2\pi i \frac{\tau k}{N}\right) = \\ = &\ \Xi_I(k) + \textstyle\sum_{n=0}^{N-1} \left[N\left(1-2\nu\right)\right] exp\left(2\pi i \frac{\tau k}{N}\right) = \\ = &\ \Xi_I(k) + N\left[N\left(1-2\nu\right)\right]\delta(k)\end{aligned}$$

where $\delta(k) = 1$ if $k = 0$ and $\delta(k) = 0$, otherwise. By evaluating the normalized version of $\Xi_I(k)$, $\overline{\Xi}_I(k) \triangleq \frac{\Xi_I(k)}{\Xi_I(0)}$, and $\Xi_C(k)$, $\overline{\Xi}_C(k) \triangleq \frac{\Xi_C(k)}{\Xi_C(0)}$, it turns out that

$$\overline{\Xi}_C(k) = \frac{\Xi_I(k)}{\Xi_I(0) + N\left[N\left(1-2\nu\right)\right]}$$

when $k \neq 0$. Consequently,

$$\Psi = \frac{\overline{\Xi}_C(k)}{\overline{\Xi}_I(k)} = \frac{\Xi_I(0)}{\Xi_I(0) + N\left[N\left(1-2\nu\right)\right]}, \quad k \neq 0.$$

Finally, since $\Xi_I(0) = \sum_{n=0}^{N-1} \xi_I(\tau) exp\,(0) = K^2$, one obtains that

$$\Psi = \frac{K^2}{K^2 + N\left[N\left(1-2\nu\right)\right]} = \frac{K^2}{K^2 + N^2 - 2NK} = \left(\frac{K}{N-K}\right)^2.$$

***- Derivation of* (12)**

The array factor of the array generated from $\mathbf{D}_I^{(\sigma)}$ is equal to [9]

$$S_I^{(\sigma)}(u) = \sum_{k=0}^{N-1} \omega_I^{(\sigma)}(k) \frac{sin\left(\pi duN - k\pi\right)}{N\, sin\left(\pi du - \frac{k\pi}{N}\right)} \tag{16}$$

where $\omega_I^{(\sigma)}(k) \triangleq IDFT\left\{w_I^{(\sigma)}(n)\right\} = \sum_{n=0}^{N-1} w_I^{(\sigma)}(n) exp(2\pi i \frac{nk}{N})$ $(k = 0, ..., N-1)$ and $w_I^{(\sigma)}(n)$ is defined as follows

$$w_I^{(\sigma)}(n) = \begin{cases} 1 & if\, n \in \mathbf{D}_I^{(\sigma)} \\ 0 & otherwise \end{cases}. \tag{17}$$

By substituting (16) into (6), one obtains

$$PSL\left(\mathbf{D}_I^{(\sigma)}\right) = \frac{max_{u \notin R_m} \left| \sum_{k=0}^{N-1} \omega_I^{(\sigma)}(k) \frac{sin(\pi duN - k\pi)}{N\, sin\left(\pi du - \frac{k\pi}{N}\right)} \right|^2}{K^2}. \tag{18}$$

As regards the lower bounds of $PSL\left(\mathbf{D}_I^{(\sigma)}\right)$, it results that

$$PSL\left(\mathbf{D}_I^{(\sigma)}\right) \geq \frac{max_{k \in \left[1, \lfloor \frac{N-1}{2} \rfloor\right]} \left|\omega_I^{(\sigma)}(k)\right|^2}{K^2} \tag{19}$$

by sampling (18) at $u = \frac{p}{Nd}$, $p = 1, ..., N-1$ and observing that $u = 0 \in R_m$. Then,

$$PSL\left(\mathbf{D}_I^{(\sigma)}\right) \geq \frac{1}{K^2} max_{k \in \left[1, \lfloor \frac{N-1}{2} \rfloor\right]} \Xi_I(k) \tag{20}$$

since [9]

$$\omega_I^{(\sigma)}(k) = \sqrt{\Xi_I(k)} exp(i\phi_k^{(\sigma)}). \tag{21}$$

By using (20), it can deduced that the lower bound PSL_{MIN}^I coincides with PSL_{MIN}^{opt} in [9] since the right term in (20) does not depend on σ.

As far as PSL_{DW}^I is concerned, a tighter bound than that in [9] can be provided. Towards this end, starting from the observation that the peaks of the beampattern within the sidelobe region are located at $u = \frac{q+1/2}{Nd}$ [9], let us consider the following approximation

$$PSL\left(\mathbf{D}_I^{(\sigma)}\right) \approx \frac{max_q \left| \sum_{k=1}^{N-1} \sqrt{\Xi_I(k)} exp(i\phi_k^{(\sigma)}) \frac{(-1)^{q-k}}{N\, sin\left[\frac{\pi}{N}\left(q-k+\frac{1}{2}\right)\right]} \right|^2}{K^2}, \quad q = 1, .., \left\lfloor \frac{N-1}{2} \right\rfloor. \tag{22}$$

If the the explicit form of the ADS $\mathbf{D}_I^{(\sigma)}$ is available, then Γ [see (13)] is a known quantity and (22) can be reformulated as follows

$$PSL\left(\mathbf{D}_I^{(\sigma)}\right) \geq \Gamma\, max_q \left| \sum_{k=1}^{N-1} exp(i\phi_k^{(\sigma)}) \frac{(-1)^{q-k}}{N\, sin\left[\frac{\pi}{N}\left(q-k+\frac{1}{2}\right)\right]} \right|^2 \quad q = 1, .., \left\lfloor \frac{N-1}{2} \right\rfloor.$$

By defining the quantity $\Delta(N) = min_{\sigma=0,..,N-1} \left\{ max_q \left| \sum_{k=1}^{N-1} exp(i\phi_k^{(\sigma)}) \frac{(-1)^{q-k}}{N\, sin\left[\frac{\pi}{N}\left(q-k+\frac{1}{2}\right)\right]} \right|^2 \right\}$ ($q = 1, .., \left\lfloor \frac{N-1}{2} \right\rfloor$), it turns out that

$$PSL\left(\mathbf{D}_I^{(\sigma)}\right) \geq \Gamma\, \Delta(N) \tag{23}$$

where the term on the right side is independent on σ. In order to estimate $\Delta(N)$ and likewise to [9], it is possible to model the phase terms $\phi_k^{(\sigma)}$ ($k = 1, .., N-1$) as independent identically distributed (i.i.d) uniform random variables. Since the statistics of $\Delta(N)$ are not known in closed form, Monte Carlo simulations were carried out to derive the following approximation

$$E\left\{\Delta(N)\right\} \approx 0.5 + 0.8\, log_{10}(N) \tag{24}$$

which holds true for $N \gtrsim 100$. By substituting (24) in (23), the analytical form of PSL_{DW}^I is obtained.

Concerning the upper bounds of $PSL\left(\mathbf{D}_I^{(\sigma)}\right)$, the following approximation can be obtained starting from (22)

$$PSL\left(\mathbf{D}_I^{(\sigma)}\right) \leq \frac{max_k \Xi_I(k)}{\Xi_I(0)} max_q \left| \sum_{k=1}^{N-1} \frac{exp(i\phi_k^{(\sigma)})(-1)^{q-k}}{N\, sin\left[\frac{\pi}{N}\left(q-k+\frac{1}{2}\right)\right]} \right|^2, \quad q = 1, .., \left\lfloor \frac{N-1}{2} \right\rfloor. \tag{25}$$

Then, after simple manipulations, it turns out that

$$PSL\left(\mathbf{D}_I^{(\sigma)}\right) \leq \frac{max_k \Xi_I(k)}{\Xi_I(0)} \mathcal{M}_{max} \tag{26}$$

where $\mathcal{M}_{max} = max_\sigma\left[\mathcal{M}(\sigma)\right]$ ($\sigma = 0, ..., N-1$) and

$$\mathcal{M}(\sigma) \triangleq max_q \left| \sum_{k=1}^{N-1} \frac{exp(i\phi_k^{(\sigma)})(-1)^{q-k}}{N\, sin\left[\frac{\pi}{N}\left(q-k+\frac{1}{2}\right)\right]} \right|^2, \quad q = 1, .., \left\lfloor \frac{N-1}{2} \right\rfloor.$$

Still modeling the phase terms $\phi_k^{(\sigma)}$ ($k = 1, .., N-1$) as i.i.d uniform random variables and performing Monte Carlo simulations, the following approximation can be obtained

$$\mathcal{M}_{max} \approx 1.9 + 1.8\, log_{10}(N), \quad N \gtrsim 100.$$

By recalling that [9]

$$\frac{max_k \Xi_I(k)}{\Xi_I(0)} \leq \frac{K - \Lambda - 1 + \sqrt{t(N-t)}}{K^2}$$

and substituting in (26), the upper bound PSL_{MAX}^I is obtained.

As for PSL_{UP}^I, one can observe that when the ADS at hand is known, χ is a known quantity. Thus, the following bound can be deduced directly from (26)

$$PSL_{UP}^I = \frac{max_k \Xi_I(k)}{\Xi_I(0)} \left[1.9 + 1.8\, log_{10}(N)\right].$$

Finally, it is worthwhile to point out that the bounds on $PSL\left(\mathbf{D}_C^{(\sigma)}\right)$ can be directly inferred from those on $PSL\left(\mathbf{D}_I^{(\sigma)}\right)$ by simple substitution of K_C and Λ_C with K and Λ, respectively, throughout the derivation. More specifically, one can deduce (12) by exploiting the relationship between $\Xi_I(k)$ and $\Xi_C(k)$ [Eq. (11)].

References

[1] Haupt, R. L.: 'Interleaved thinned linear arrays,' *IEEE Trans. Antennas Propag.*, 2005, 53, (9), pp. 2858-2864.

[2] Haupt, R. L., and Werner, D. H.: 'Genetic algorithms in electromagnetics' (Hoboken, NJ: Wiley, 2007).

[3] Hsiao, J.: 'Analysis of interleaved arrays of waveguide elements,' *IEEE Trans. Antennas Propag.*, 1971, 19, pp. 729-735.

[4] Boyns, J., and Provencher, J.: 'Experimental results of a multifrequency array antenna,' *IEEE Trans. Antennas Propag.*, 1972, 20, pp. 106-107.

[5] Stangel, J., and Punturieri, J.: 'Random subarray techniques in electronic scan antenna design,' *Proc. IEEE AP-S Symp.*, Dec. 1972, pp. 17-20.

[6] D'Urso, M., and Isernia, T.: 'Solving some array synthesis problems by means of an effective hybrid approach,' *IEEE Trans. Antennas Propag.*, 2007, 55, pp. 106-107.

[7] Ding, C., Helleseth, T., and Lam, K. Y.: 'Several classes of binary sequences with three-level autocorrelation,' *IEEE Trans. Inf. Theory*, 1999, 45, (7), pp. 2606-2612.

[8] Leeper, D. G.: 'Isophoric arrays - massively thinned phased arrays with well-controlled sidelobes,' *IEEE Trans. Antennas Propag.*, 1999, 47, (12), pp. 1825-1835.

[9] Oliveri, G., Donelli, M., and Massa, A.: 'Linear array thinning exploiting almost difference sets,' *IEEE Trans. Antennas Propag.*, 2009, 57, (12), pp. 3800-3812.

[10] Arasu, K. T., Ding, C., Helleseth, T., Kumar, P. V., and Martinsen, H. M.: 'Almost difference sets and their sequences with optimal autocorrelation,' *IEEE Trans. Inf. Theory*, 2001, 47, (7), pp. 2934-2943.

[11] ELEDIA Almost Difference Set Repository (*http://www.eledia.ing.unitn.it/*).

[12] Zhang, Y., Lei, J. G., and Zhang, S. P.: 'A new family of almost difference sets and some necessary conditions,' *IEEE Trans. Inf. Theory*, 2006, 52, (5), pp. 2052-2061.

[13] Balanis, C. A.: ’Antenna Theory: Analysis and Design’ (New York: Wiley, 1997).

[14] Oliveri G., Manica L., and Massa A., “On the impact of mutual coupling effects on the PSL performances of ADS thinned arrays”, *Progress in electromagnetic research B*, 2009, 17, pp. 293-308.

[15] King, H., and Wong, J.: ’Directivity of a uniformly excited N X N array of directive elements,’ *IEEE Trans. Antennas Propag.*, 1975, 23, (4), pp. 401-404.

FIGURE CAPTIONS

- **Figure 1.** *Balanced interleaved arrays* [$N = 30$, $\nu = 0.5$, $\eta = 0.75$ - $(30, 15, 7, 22)$-ADS]: (*a*) binary sequences and interleaved arrangement, (*b*) plots of $\xi_I(\tau)$ and $\xi_C(\tau)$, and (*c*) plots of $|S_I(u)|^2$, $|S_C(u)|^2$, $\Xi_I(k)$, and $\Xi_C(k)$.

- **Figure 2.** *Unbalanced interleaved arrays* [$N = 53$, $\nu = 0.264$, $\eta = 0.25$ - $(53, 14, 3, 26)$-ADS]: (*a*) binary sequences and interleaved arrangement, (*b*) plots of $\xi_I(\tau)$ and $\xi_C(\tau)$, and (*c*) plots of $|S_I(u)|^2$, $|S_C(u)|^2$, $\Xi_I(k)$, and $\Xi_C(k)$.

- **Figure 3.** Plot of Ψ versus ν.

- **Figure 4.** *Balanced interleaved arrays* [$N = 150$ (aperture size: 74.5λ), $\nu = 0.5$, $\eta = 0.75$ - $(150, 75, 37, 112)$-ADS]: (*a*) PSL value versus cyclic shift σ, $\sigma = 0, ..., N-1$. Plots of the normalized patterns $|S_I(u)|^2$ and $|S_C(u)|^2$ generated from (*b*) $\mathbf{D}_I^{(\sigma^{comp})}$, (*c*) $\mathbf{D}_I^{(\sigma_I^{opt})}$, and (*d*) $\mathbf{D}_I^{(\sigma_C^{opt})}$.

- **Figure 5.** *Balanced interleaved arrays* [$N = 700$ (aperture size: 349.5λ), $\nu = 0.5$, $\eta = 0.25$ - $(700, 350, 174, 175)$-ADS]: (*a*) PSL value versus the cyclic shift σ, $\sigma = 0, ..., N-1$. Plots of the normalized patterns $|S_I(u)|^2$ and $|S_C(u)|^2$ generated from (*b*) $\mathbf{D}_I^{(\sigma^{comp})}$, (*c*) $\mathbf{D}_I^{(\sigma_I^{opt})}$, and (*d*) $\mathbf{D}_I^{(\sigma_C^{opt})}$.

- **Figure 6.** *Balanced interleaved arrays* [$\nu = 0.5$, $\eta = 0.25$]: (*a*) representative points of the ADS-based solutions and PSL bounds when $N = 150$, $N = 312$, $N = 700$, and (*b*) PSL values and bounds versus the array size N.

- **Figure 7.** *Unbalanced interleaved arrays* [$\nu = 0.25$, $\eta = 0.5$]: (*a*) representative points of the ADS-based solutions and PSL bounds when $N = 149$, $N = 349$, $N = 701$, (*b*) PSL^I and (*c*) PSL^C values and bounds versus the array size N.

- **Figure 8.** *Unbalanced interleaved arrays* [$\nu = 0.25$, $\eta = 0.5$]. Plots of the normalized patterns $|S_I(u)|^2$ and $|S_C(u)|^2$ generated from the σ^{comp}-th shifted version of (*a*) the $(149, 38, 9, 74)$-ADS ($N = 149$ - Aperture size: 74λ) and (*c*) the $(701, 175, 43, 350)$-ADS ($N = 701$ - Aperture size: 350λ).

- **Figure 9.** Element pattern of the directive radiator for different values of the "directivity" index m [$m \in \{0,\ 0.25,\ 1,\ 10,\ 99,\ 200,\ 300\}$].

- **Figure 10.** *Unbalanced interleaved arrays* [$N = 106$, $\nu = 0.49$, $\eta = 0.75$]: (*a*) PSL value versus the cyclic shift σ, $\sigma = 0, ..., N-1$, (*b*) representative points of the ADS-based solutions with isotropic and directive elements ($m = 0.25$), and (*c*) plots of the normalized patterns $|S_C(u)|^2$ and $\left|S_I^{(m)}(u)\right|^2$ ($m = 0.0,\ 0.25$) in correspondence with $\mathbf{D}_I^{(\sigma_m^{comp})}$.

- **Figure 11.** *Unbalanced interleaved arrays* [$N = 109$, $\nu = 0.25$, $\eta = 0.5$]: (*a*) PSL value versus the cyclic shift σ, $\sigma = 0, ..., N-1$, (*b*) representative points of the ADS-based solutions with isotropic and directive elements ($m = 10,\ 300$), and (*c*) plots of the normalized patterns $|S_C(u)|^2$ and $\left|S_I^{(m)}(u)\right|^2$ ($m = 0,\ 10,\ 300$) in correspondence with $\mathbf{D}_I^{(\sigma_m^{comp})}$.

- **Figure 12.** *Comparative Assessment - Balanced interleaved arrays* [$N = 109$ (aperture size: 29.5λ), $\nu = 0.5$]: (*a*) PSL value of the GA solution [1] and the ADS-based array versus the cyclic shift σ, $\sigma = 0, ..., N-1$, (*b*) representative points, and (*c*) plots of the normalized patterns derived from the ADS $\mathbf{D}^{(\sigma^{comp})}$ and synthesized by the GA-based procedure.

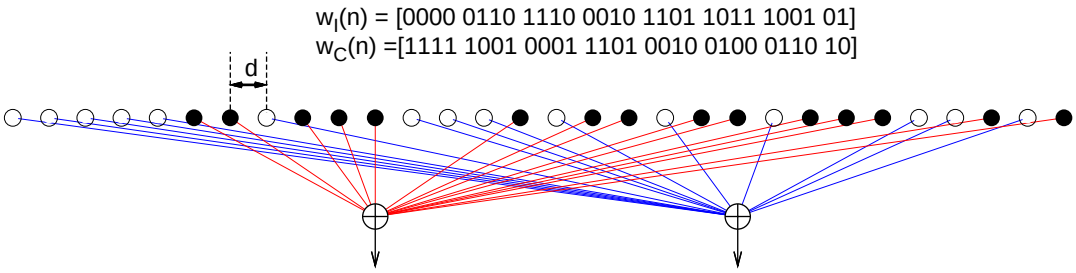

(*a*)

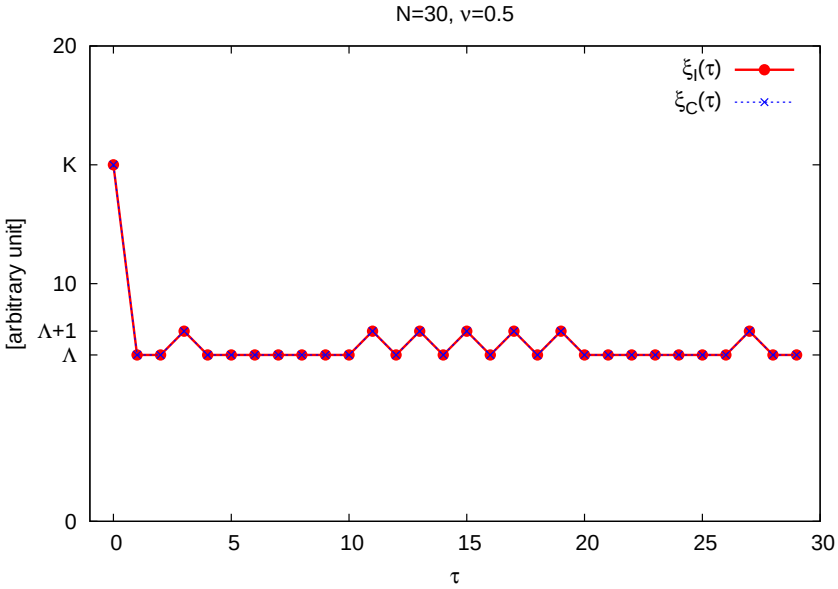

(*b*)

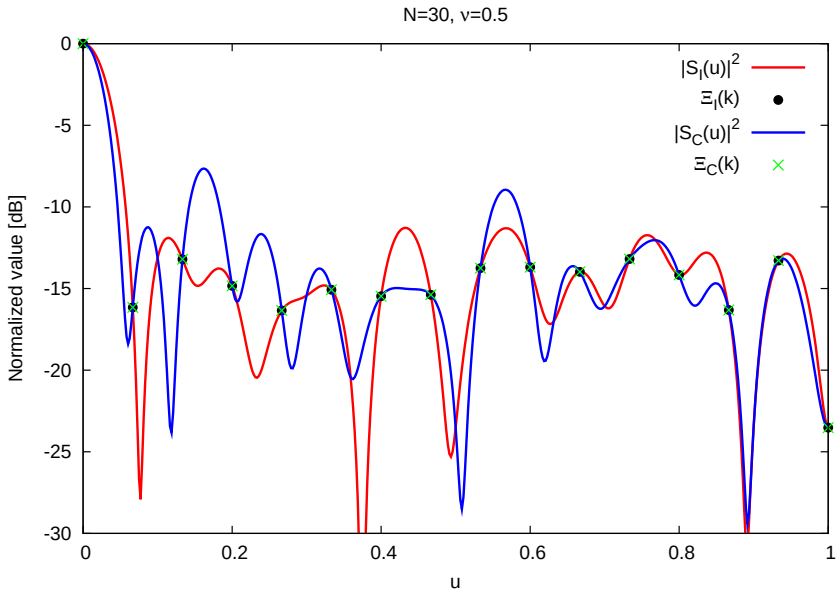

(*c*)

Figure 1 - G. Oliveri et *al.*, "Fully-Interleaved Linear Arrays ..."

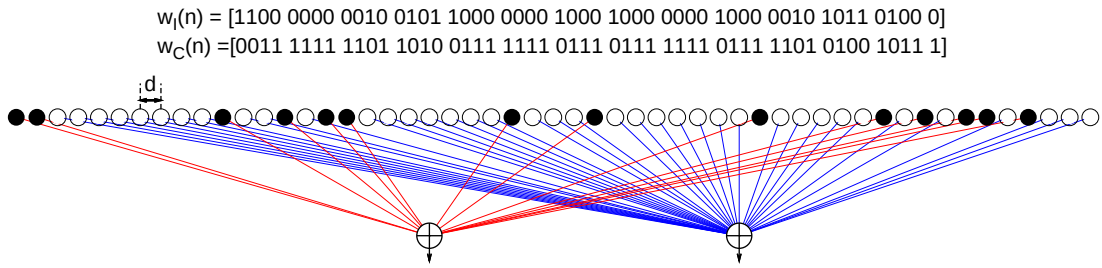

(*a*)

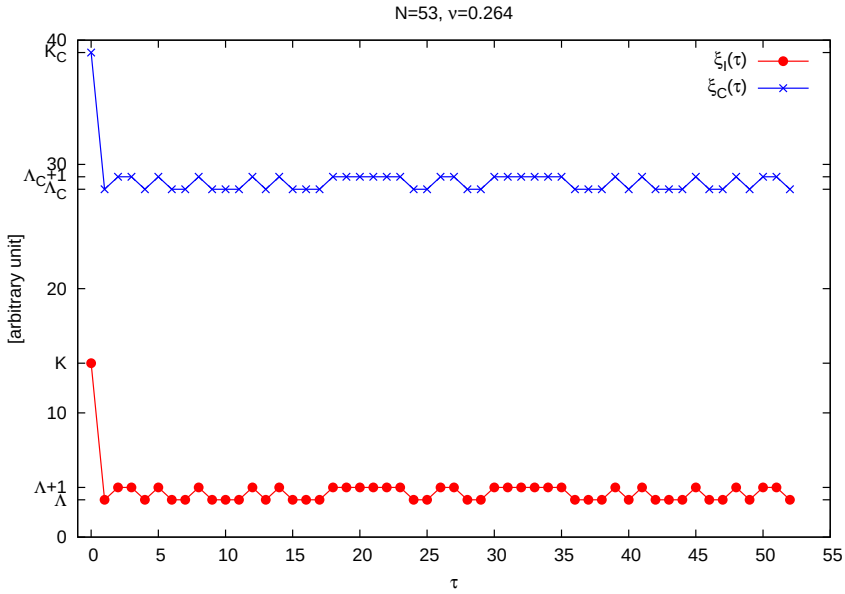

(*b*)

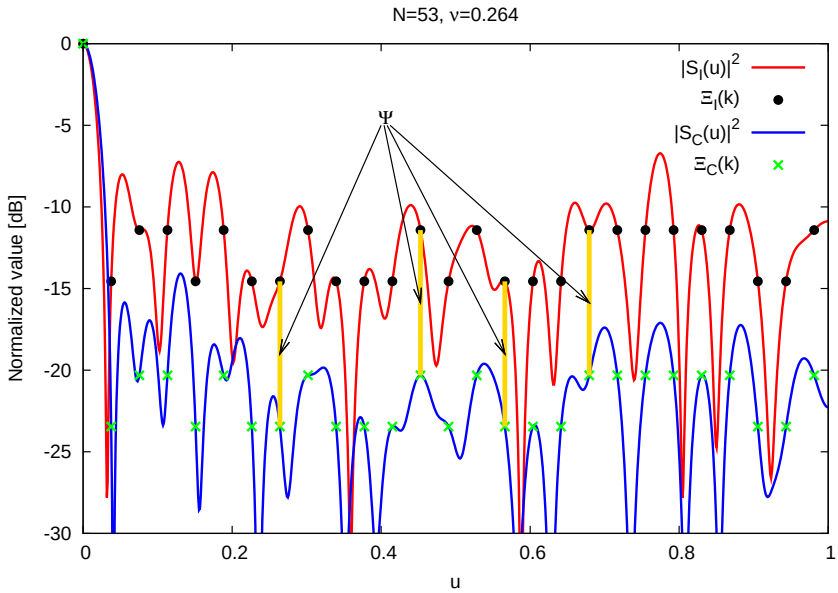

(*c*)

Figure 2 - G. Oliveri et *al.*, "Fully-Interleaved Linear Arrays ..."

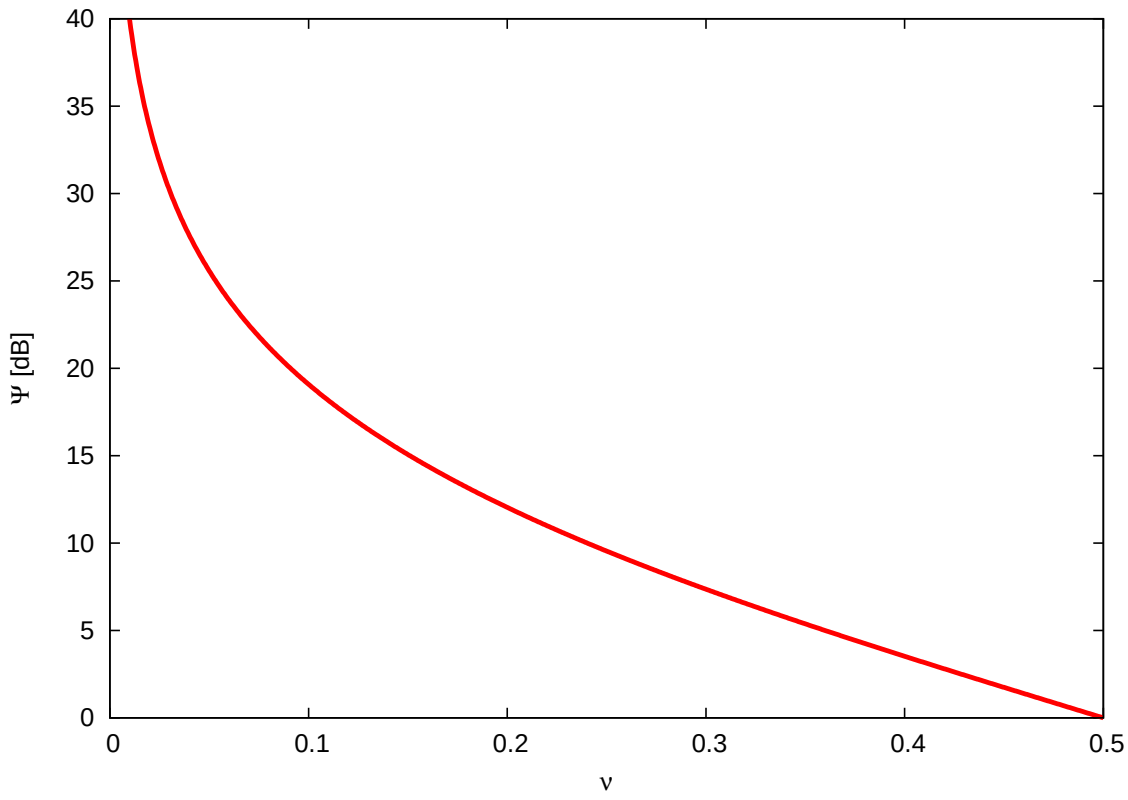

Figure 3 - G. Oliveri et *al.*, “Fully-Interleaved Linear Arrays ...”

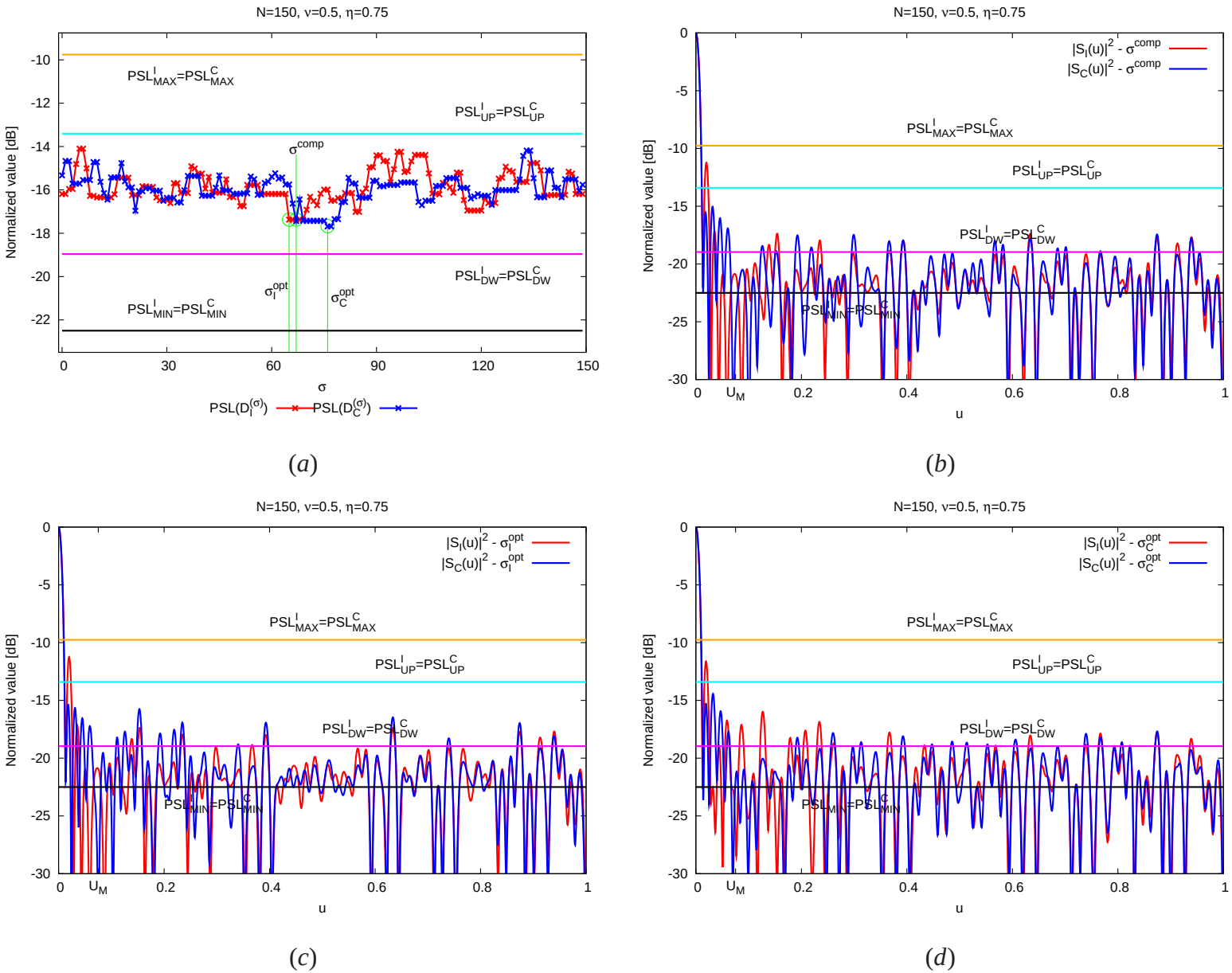

Figure 4 - G. Oliveri et *al.*, "Fully-Interleaved Linear Arrays ..."

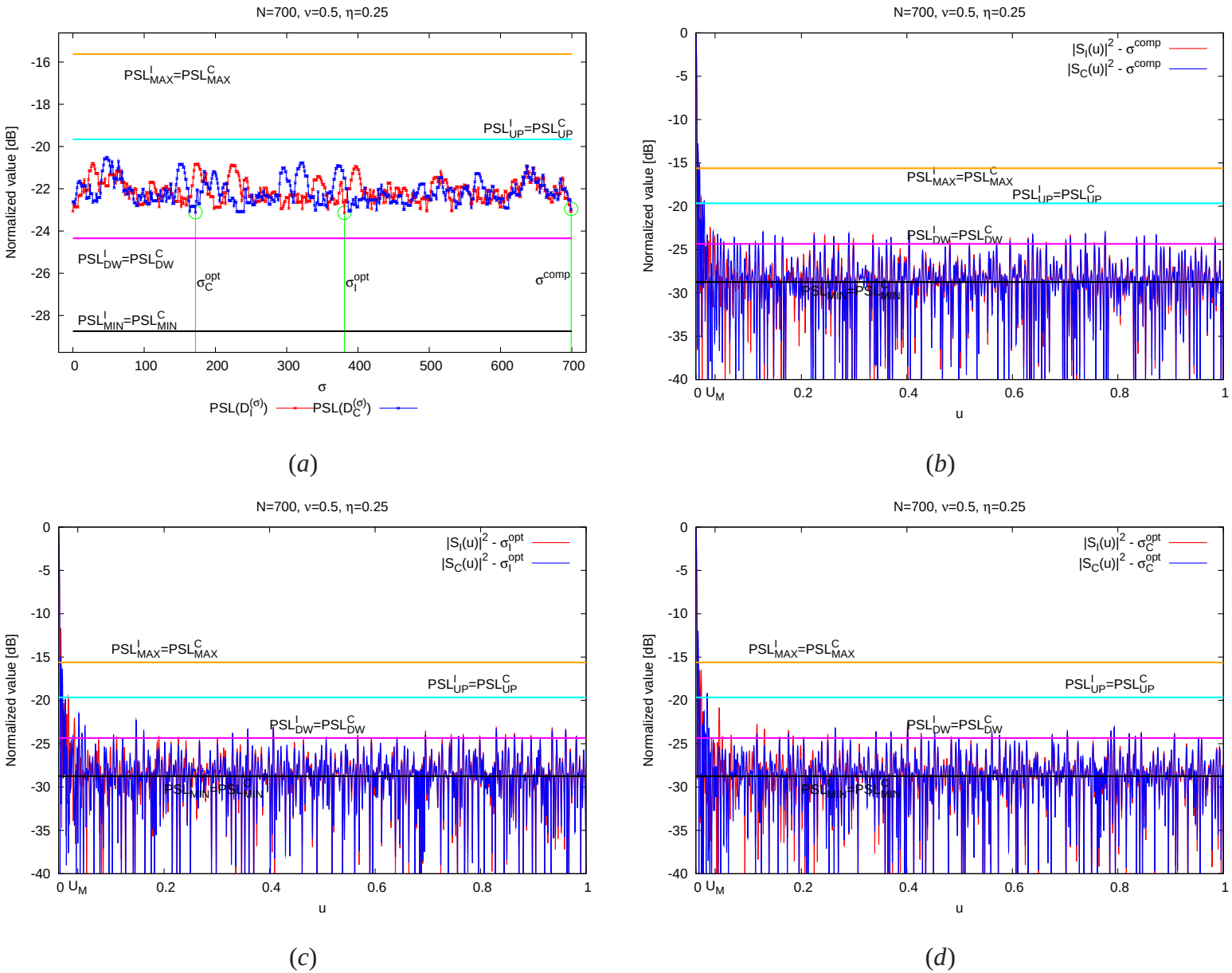

(*a*) (*b*) (*c*) (*d*)

Figure 5 - G. Oliveri et *al.*, "Fully-Interleaved Linear Arrays ..."

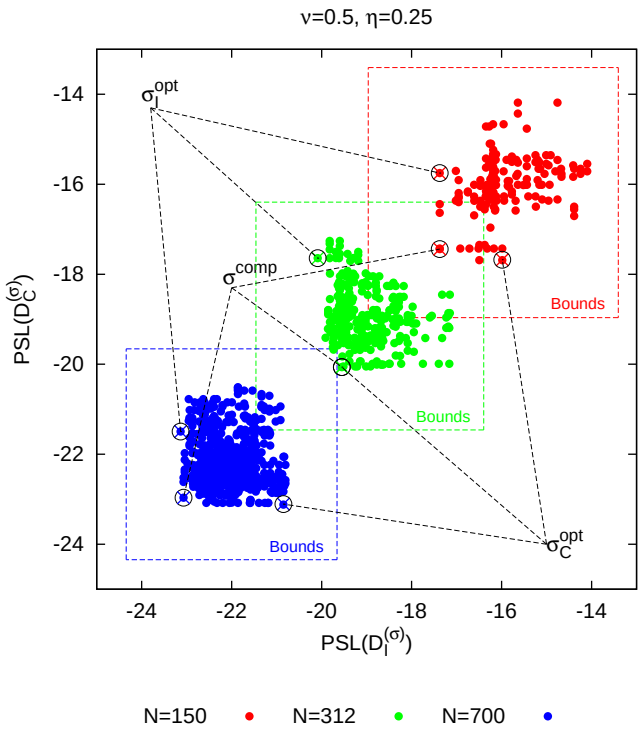

(*a*)

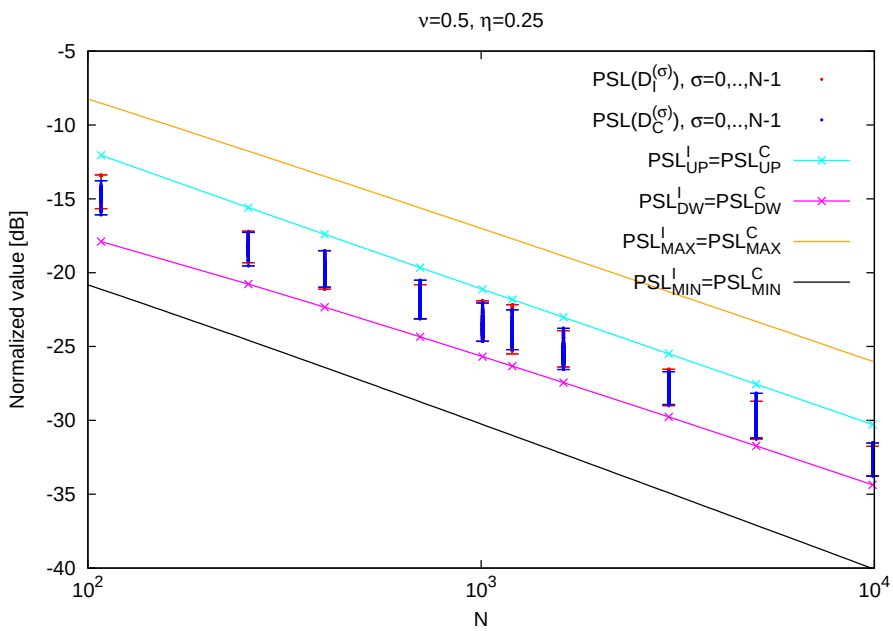

(*b*)

Figure 6 - G. Oliveri et *al.*, "Fully-Interleaved Linear Arrays ..."

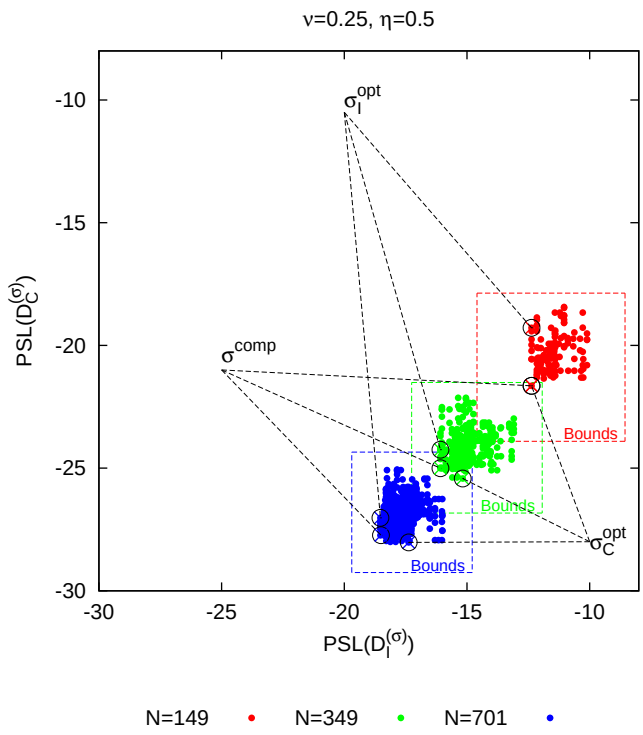

(*a*)

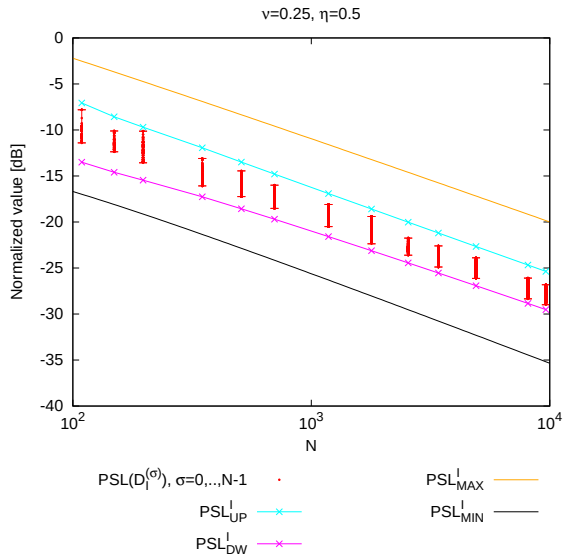

(*b*)

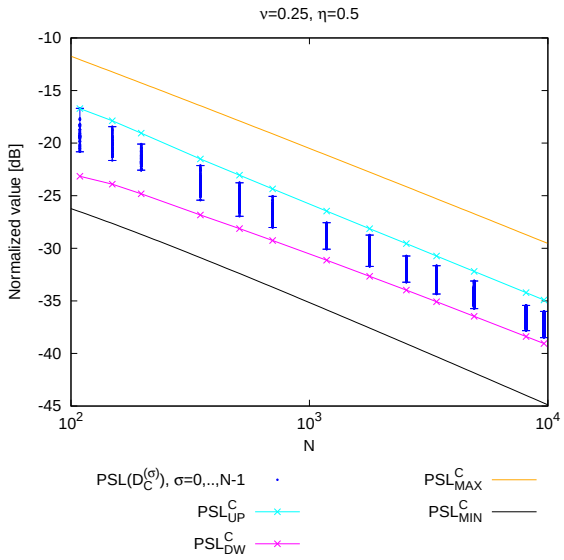

(*c*)

Figure 7 - G. Oliveri et *al.*, "Fully-Interleaved Linear Arrays ..."

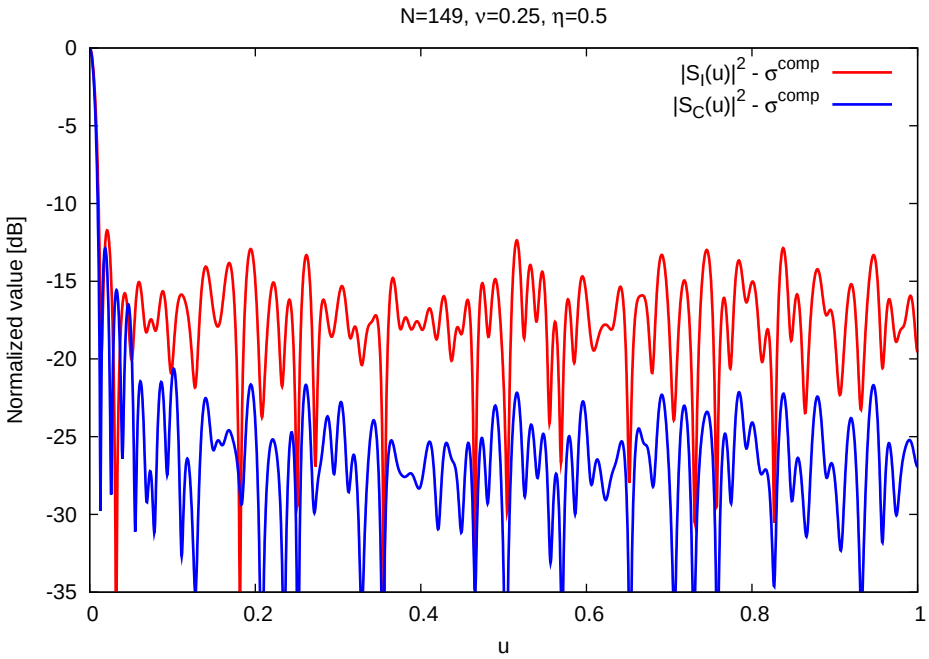

(*a*)

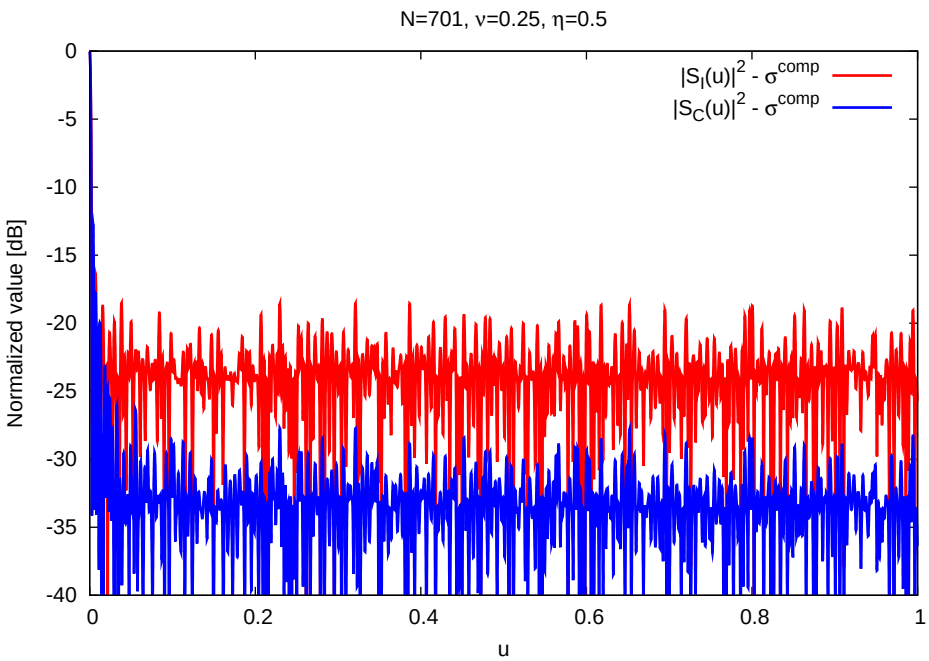

(*b*)

Figure 8 - G. Oliveri et *al.*, "Fully-Interleaved Linear Arrays ..."

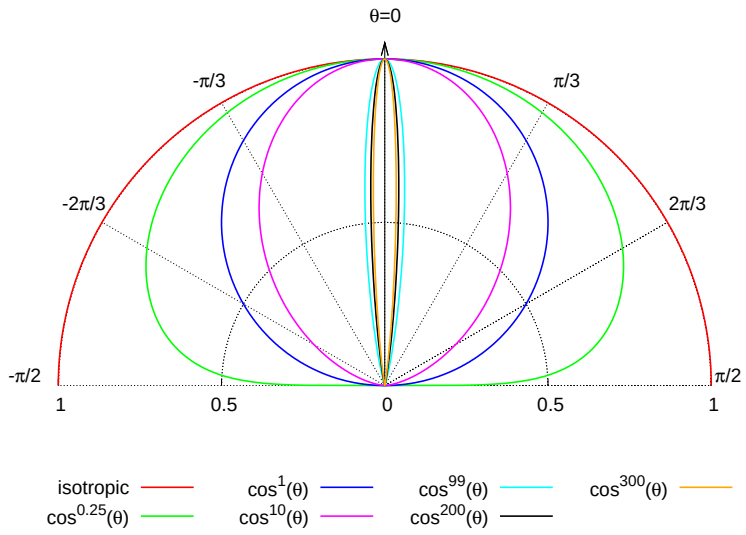

Figure 9 - G. Oliveri et *al.*, "Fully-Interleaved Linear Arrays ..."

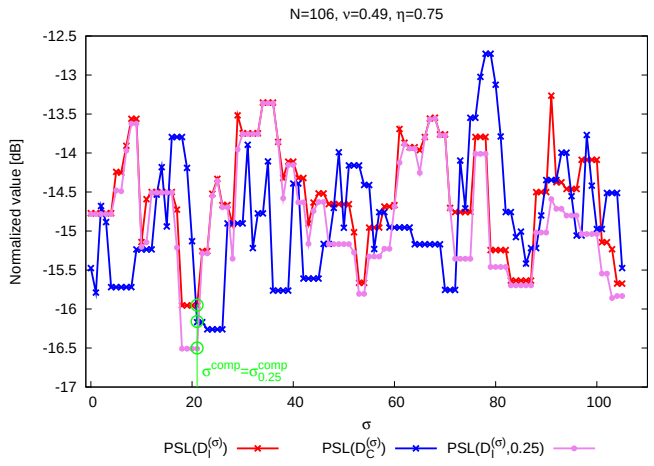

(*a*)

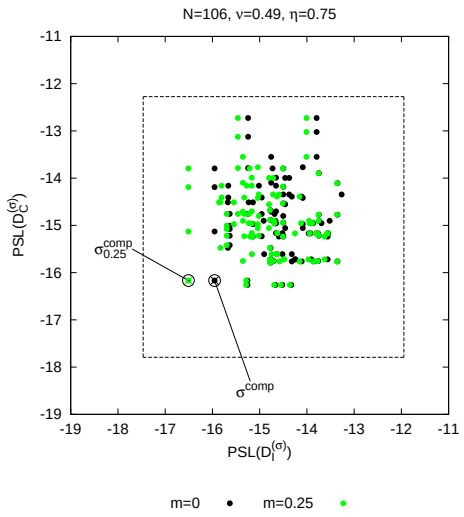

(*b*)

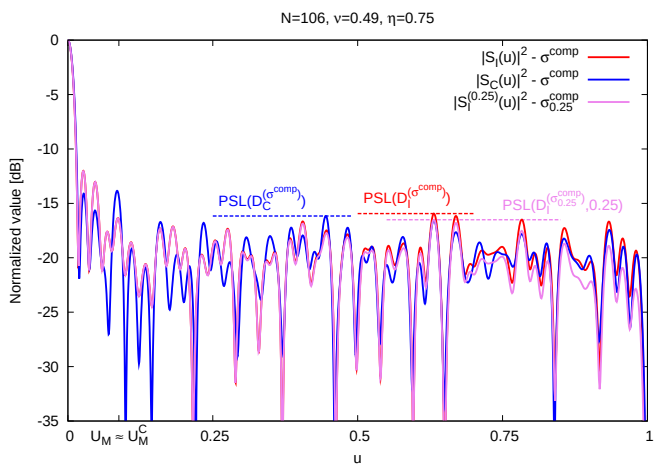

(*c*)

Figure 10 - G. Oliveri et *al.*, “Fully-Interleaved Linear Arrays ...”

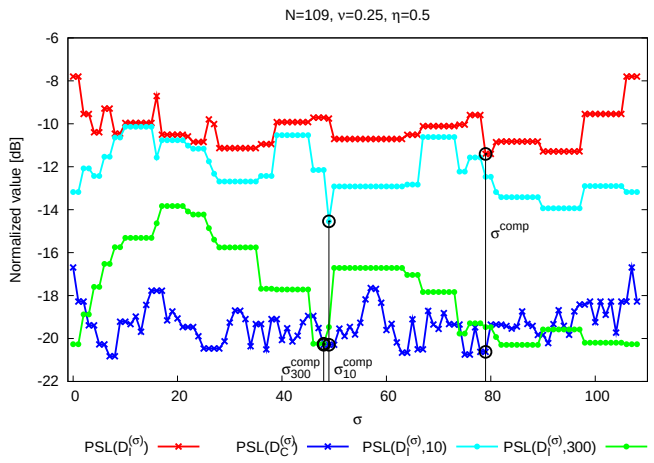

(*a*)

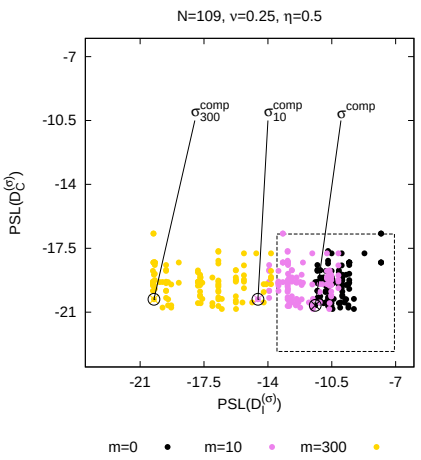

(*b*)

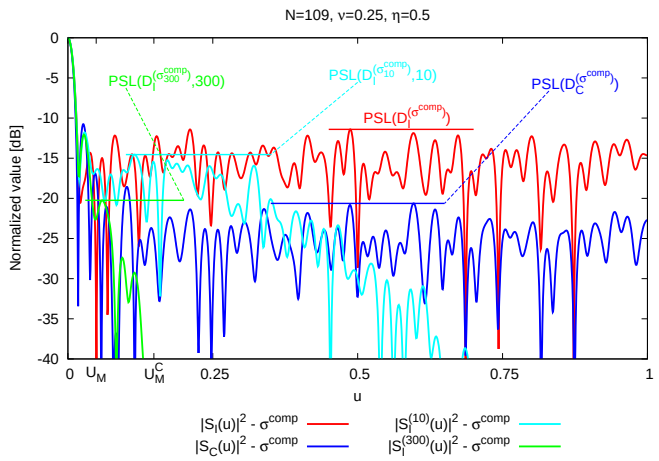

(*c*)

Figure 11 - G. Oliveri et *al.*, “Fully-Interleaved Linear Arrays ...”

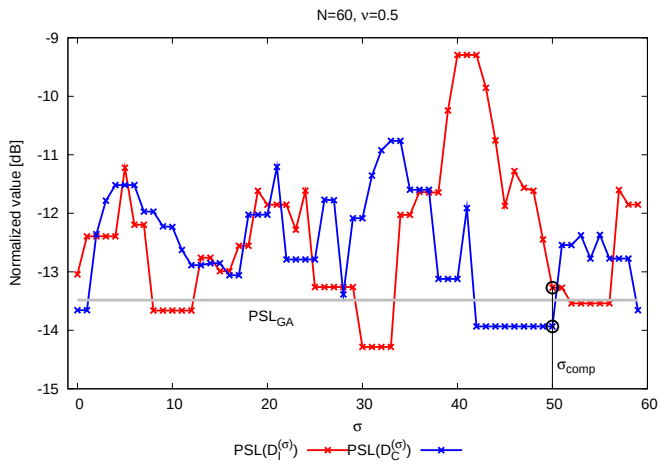

(*a*)

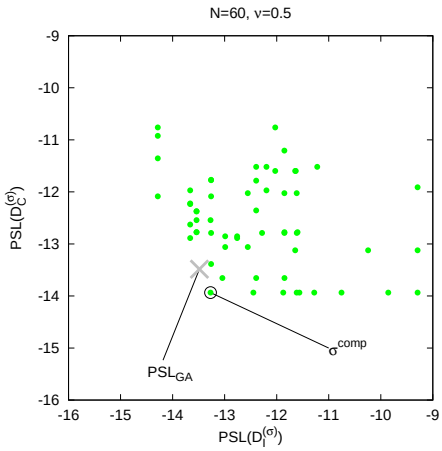

(*b*)

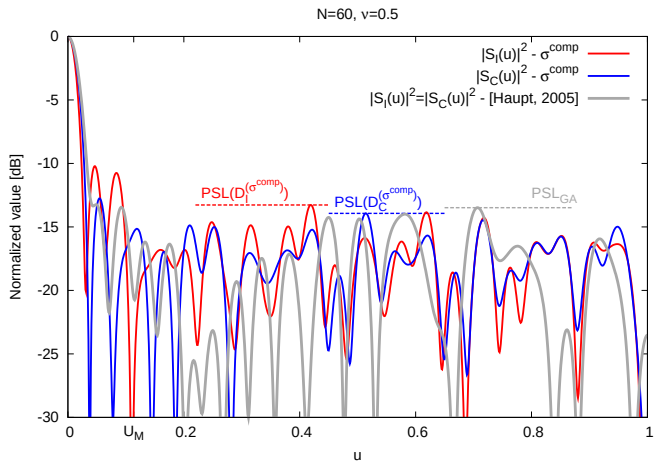

(*c*)

Figure 12 - G. Oliveri et *al.*, “Fully-Interleaved Linear Arrays ...”